

# Growth and electronic structure of 1,10-phenanthroline ultra-thin films on Au(111) as a model catalyst for the oxygen reduction reaction

Erlina TIK MAN<sup>1</sup>, Yuya KANEKO<sup>1</sup>, Ryunosuke KOBATA<sup>1</sup>, Takaya SHIMOKAWA<sup>1</sup>,  
Tzu-YEN CHEN<sup>1</sup>, Yukiko OBATA<sup>1</sup>, Kazutoshi SHIMAMURA<sup>1</sup>,  
Junji NAKAMURA<sup>2</sup>, and Yasuo YOSHIDA<sup>1\*</sup>

<sup>1</sup>Department of Physics, Kanazawa University, Kanazawa 920-1192, Japan

<sup>2</sup>International Institute for Carbon-Neutral Energy Research (I2CNER), Kyushu University,  
Fukuoka 819-0395, Japan

(Received August 7, 2025 and accepted in revised form August 25, 2025)

**Abstract** Nitrogen-doped carbon materials containing pyridinic nitrogen (pyri-N) have emerged as promising functional materials for a variety of applications, including metal-free oxygen reduction reaction (ORR) catalysis and selective CO<sub>2</sub> adsorption, yet the role of spin-polarized unpaired electrons in their activity remains elusive. Here we report an atomic-scale investigation of a pyridinic-nitrogen-containing molecular catalyst, 1,10-Phenanthroline (1,10-phen), evaporated under ultra-high vacuum conditions onto an Au(111) surface using scanning tunneling microscopy and spectroscopy. We observe well-ordered self-assembly of molecules and randomly distributed molecular clusters, which lie flat on the surface, exposing the nitrogen sites, unlike previous studies in which the molecules stand on the Au(111) surface with the nitrogen sites down. Tunneling spectroscopy shows a distinct gap between the highest occupied and the lowest unoccupied molecular orbitals which roughly matches to the calculated gap, indicating minimal electronic disturbance upon adsorption. Ex-situ X-ray photoelectron spectroscopy confirms the existence of the 1,10-phen molecular film on Au(111) surface. The results demonstrate that vacuum deposited 1,10-phen molecular films on the Au(111) surface are promising model catalysts for investigating the ORR mechanism not only in-situ measurements such as scanning tunneling microscopy and spectroscopy but also in other ex-situ measurements.

**Keywords.** Carbon catalysts, molecular adsorption, oxygen reduction reaction

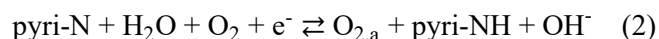
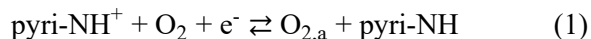
## 1 Introduction

Nitrogen-doped carbon materials have attracted considerable attention in a wide range of applications, including electrocatalysis, gas adsorption, and energy storage, due to their tunable electronic structures and the potential of low-cost synthesis<sup>[1–10]</sup>. Among these applications, their use as metal-free catalysts for the oxygen reduction reaction (ORR) in fuel cells and metal-air batteries is particularly significant. Recent studies have demonstrated that, in carbon materials containing pyridinic nitrogen (pyri-N), the electron transfer is accompanied by a concerted adsorption of

---

\* Corresponding author E-mail: yyoshida@se.kanazawa-u.ac.jp

oxygen molecules, occurring under both acidic and alkaline conditions<sup>[11][12][13]</sup>, where  $O_{2,a}$  denoted the adsorbed  $O_2$  molecule on the carbon atom next to pyri-N. In this mechanism, electrons are injected into the  $\pi^*$  orbital of pyri-N, generating a spin-polarized unpaired electron, which interacts with  $O_2$  to form a bonding orbital, thereby facilitating molecular adsorption.



The potential impact of the unpaired electron's energy level and delocalization on  $O_2$  adsorption has been pointed out in recent studies, emphasizing the importance of this factor<sup>[14][15]</sup>. However, its detailed role remains largely unresolved. Similar questions arise in  $CO_2$  adsorption, where pyri-N also functions as a selective and reversible adsorption site due to its strong Lewis basicity<sup>[16]</sup>. Although chemisorption with adsorption energies exceeding 100 kJ/mol has been reported, the detailed electronic structure contributions, especially involving the unpaired electron state, are still unclear.

To clarify the correlation between the molecular structure of pyri-N and its electronic reactivity at the atomic scale, structurally well-defined model systems are essential. The 1,10-Phenanthroline (1,10-phen), a heteroaromatic compound containing two pyri-N sites ( $C_{12}H_8N_2$ ) as shown in Fig. 1, is known to exhibit high ORR activity when supported on carbon<sup>[11][12]</sup>. However, conventional solution-based film formation leads to molecular aggregation, causing the nitrogen sites to become buried and hindering direct investigation of the reaction mechanism<sup>[17]</sup>.

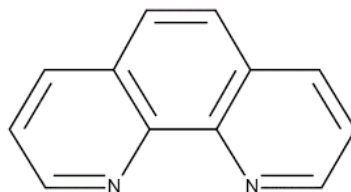


Figure 1. Chemical formula of 1,10-phenanthroline ( $C_{12}H_8N_2$ )

In this study, we employed vapor deposition under ultra-high vacuum (UHV) to deposit 1,10-phen on an Au(111) surface, forming flat molecular arrangements with exposed nitrogen sites. This approach enabled detailed analysis of structural and electronic properties using scanning tunneling microscopy/spectroscopy (STM/STS). Our STM/STS results show that the 1,10-phen molecules are physisorbed via weak van der Waals interactions with the substrate and exhibit a different formation mode than the conventional method. Furthermore, ex-situ X-ray photoelectron spectroscopy (XPS) confirms that the molecular film persists on the Au(111) surface. This work lays the foundation for future studies aimed at exploring the proposed spin-related ORR mechanism at the atomic scale.

## 2 Method

The experiments were carried out using a low-temperature, UHV scanning tunneling microscope (STM), Unisoku USM-1300 equipped with an RHK R9 controller. For both imaging and spectroscopic measurements, we used electrochemically etched tungsten tips, which were subsequently annealed in situ via electron bombardment  $\sim 1800^\circ\text{C}$ . We evaluated W tips with a clean Au(111) surface by imaging the herringbone structures and observing the onset of the Shockley surface state at  $\sim 400$  mV in the differential tunneling conductance ( $dI/dV$ ) spectroscopy. Commercial epitaxial Au(111) thin films on mica substrates (200 nm thickness; PHASIS Sàrl,

Neuchâtel, Switzerland) were cleaned in ultrahigh vacuum by repeated cycles of  $\text{Ar}^+$  sputtering and annealing at  $\sim 600^\circ\text{C}$  in a preparation chamber. The molecule used in the experiment was 1,10-phenanthroline (Wako) with a purity of 97% (confirmed by NMR). After confirming the characteristic herringbone reconstruction of the Au(111) surface via STM, we evaporated the 1,10-phen molecules onto the Au(111) substrate at room temperature using a homemade molecular evaporator heated at  $\sim 60^\circ\text{C}$  for a few seconds. After the deposition, the sample was transferred to the STM. All STM/STS measurements were performed at the sample and tip temperatures of 5.7 K and 77 K and in an ultra-high-vacuum chamber (base pressure of  $5.0 \times 10^{-8}$  Pa). The  $dI/dV$  spectra were taken using a standard lock-in method. The X-ray photoelectron spectroscopy (XPS) measurements were performed using a JEOL (JPS-9010TR) instrument with an  $\text{Mg K}\alpha$  source, and the pass energy was set to 20 eV. For the XPS data, the C 1s spectra were corrected so that the peak tops correspond to the literature value of 284.6 eV for the binding energy, and then the correction is also applied to the N 1s spectrum.

### 3 Results and discussion

#### 3.1 Structures of 1,10-phenanthroline molecular thin film

As shown in Fig. 2(a), the molecules self-assemble into a two-dimensional long-range ordered structure, which is composed of one-dimensional (1D) chain-like structure. Closer inspection

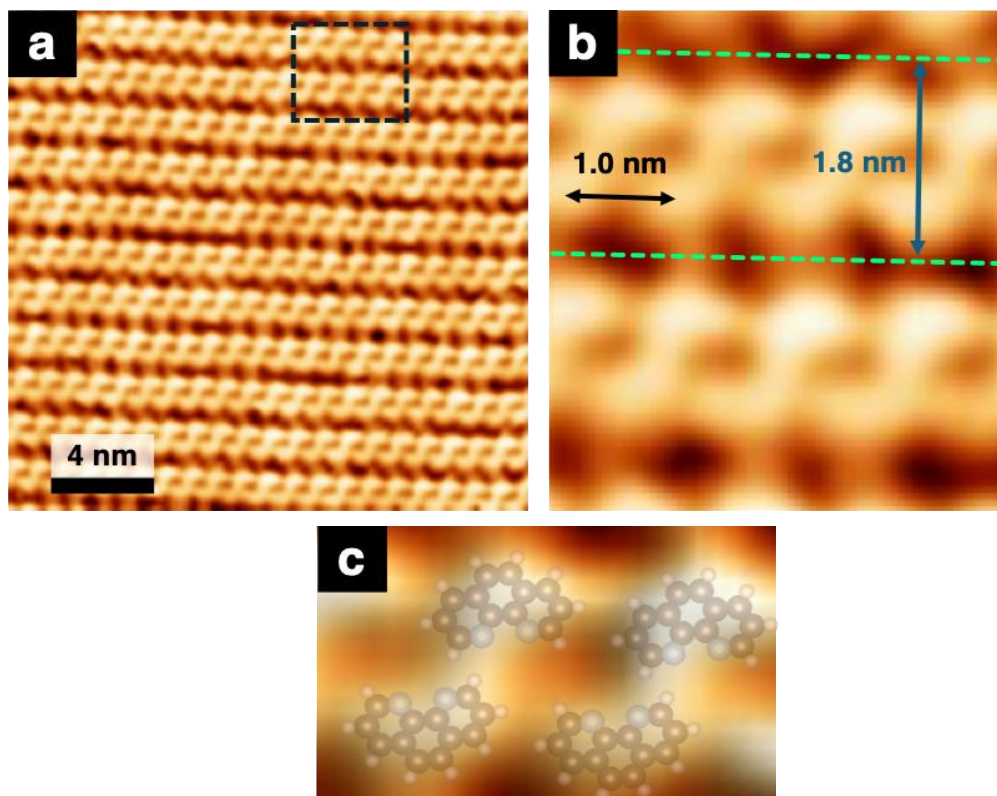


Figure 2. (a) STM image of 1,10-Phen deposited on Au(111) surface acquired at 5.7 K ( $V = 100$  mV,  $I_t = 150$  pA,  $20\text{ nm} \times 20\text{ nm}$ ). (b) Close-up STM image of (a) inside black dashed square, showing molecular dimers forming chain structure. (c) Zoomed image superimposed with a chemical formula of 1,10-phen. The corresponding 1,10-phen molecules are superimposed with a molecular model created with Visualization for Electronic and Structural Analysis.

reveals that each chain is constructed from a repeating S-shaped feature, with an inter-dimer spacing of approximately 1.0 nm along the chain direction and an inter-chain separation of  $\sim 1.8$  nm (Fig. 2(b)). By comparing with the molecular geometry, the S-shaped feature can be assigned to a dimer of two molecules lying flat on the surface as shown in Fig. 2(c). In this configuration, the nitrogen atoms of neighboring molecules are oriented toward one another. This arrangement suggests that the formation of dimers, stabilized by intermolecular CH–N hydrogen bonding, serves as the fundamental structural unit of the 1D chains.

We also observed two distinct adsorption structures on the Au(111) surface: ordered one-dimensional chains and randomly oriented molecular clusters shown in Figs. 3(a) and (b), respectively. Line profiles are along the dashed blue line on the dimer in Fig. 3(a) and the black dashed line on the cluster in Fig. 3(b). The line profile on the dimer shows a double-peak feature with the peak heights of  $\sim 0.9$  Å while one on the cluster shows a triple-peak feature with the peak heights with  $\sim 0.9$  Å,  $\sim 1.0$  Å and  $\sim 0.9$  Å. This suggests that the center molecule in the cluster, marked with a red circle, is slightly tilted, while the surrounding molecules adopt a flat-lying configuration similar to that of the dimer.

Previous studies have reported the vertical adsorption of 1,10-phen molecules on Au(111), with the nitrogen atoms facing the surface<sup>[17–19]</sup>, but their STM images are significantly different from those observed in our study. Solution-based adsorption often involves interactions between the target molecule and the molecules in the solution, as well as between the target molecule and the surface. Conversely, molecule–substrate interactions dominate the vacuum evaporation method since no other molecules or impurities exist in principle. Our results indicate that the flat-lying configuration is energetically favorable when molecule–substrate interactions dominate. The vacuum evaporation

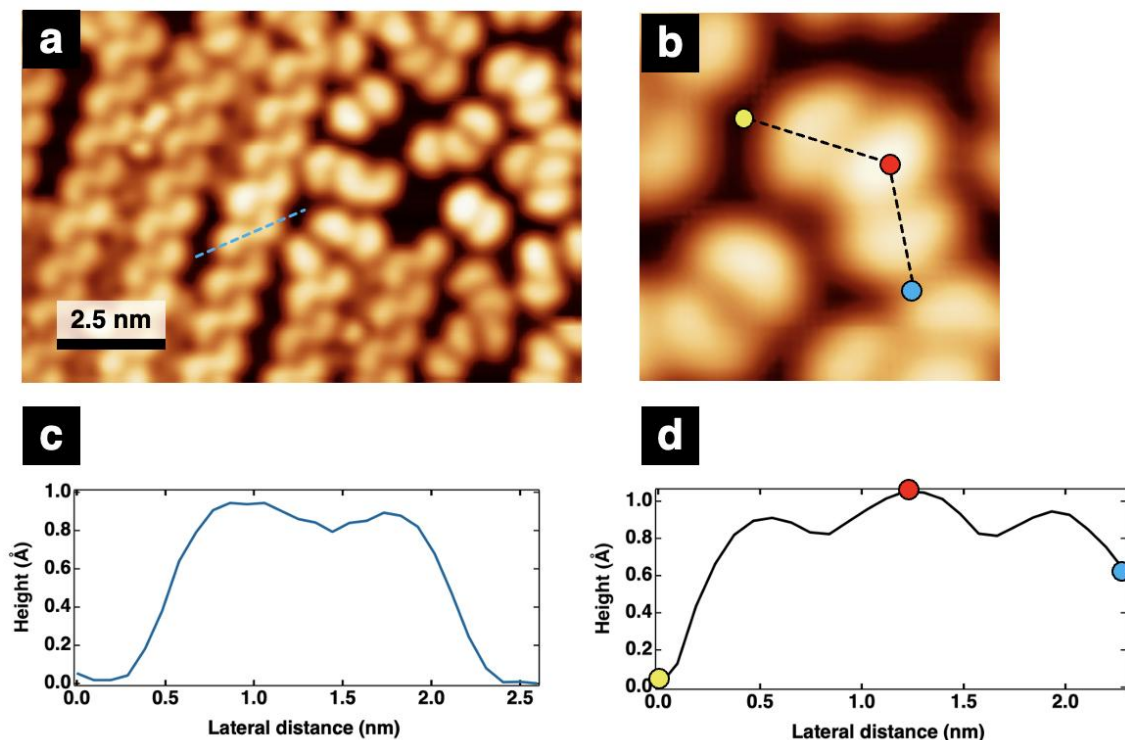


Figure 3. (a) STM images of 1,10-phen/Au(111) showing a coexistence of chain structure and randomly oriented molecular cluster, (b) Zoomed-in image of a molecular cluster, (c) Line profile along the blue dashed line in (a), (d) Line profile along the black dashed line in (b).

method provides direct access to pyridinic nitrogen sites, making it highly suitable for microscopic studies that clarify ORR activity, and offering a more realistic and functional platform for investigating the origin of ORR around pyridinic nitrogen sites.

### 3.2 Tunneling spectroscopy

To elucidate the electronic interactions between 1,10-phen and the Au(111) substrate, we measured tunneling spectra on top of molecule, as shown in Fig. 4. The two distinct peaks in the  $dI/dV$  signal appear around -2.1 V and +2.1 V, which we attribute to the highest occupied molecular orbital (HOMO) and the lowest unoccupied molecular orbital (LUMO) peak, respectively. The resulting HOMO-LUMO energy gap of approximately 4.2 eV is in reasonable agreement with the theoretical calculations of an isolated 1,10-phen around 4.8 eV<sup>[18]</sup>, suggesting that the adsorption effect on Au(111) is less significant.

In addition to the HOMO and LUMO peaks, step-like or peak-like features are observed in the vicinity of the fermi level  $E_F$ . For the reference, we also show the step-like feature of the Shockley surface state taken on a bare Au(111) substrate, which has an onset at  $\sim -400$  mV. On the molecular layer, the  $dI/dV$  starts increasing at -500 mV but less steep compared with that of a bare Au(111), and a step appears around -300 mV followed by a broad peak at -60 mV. Similar to the case of picene on Ag(111)<sup>[19]</sup>, the surface state persists after adsorption, indicating negligible hybridization and charge transfer between the substrate s-derived states and the molecular orbitals, and thus a weak

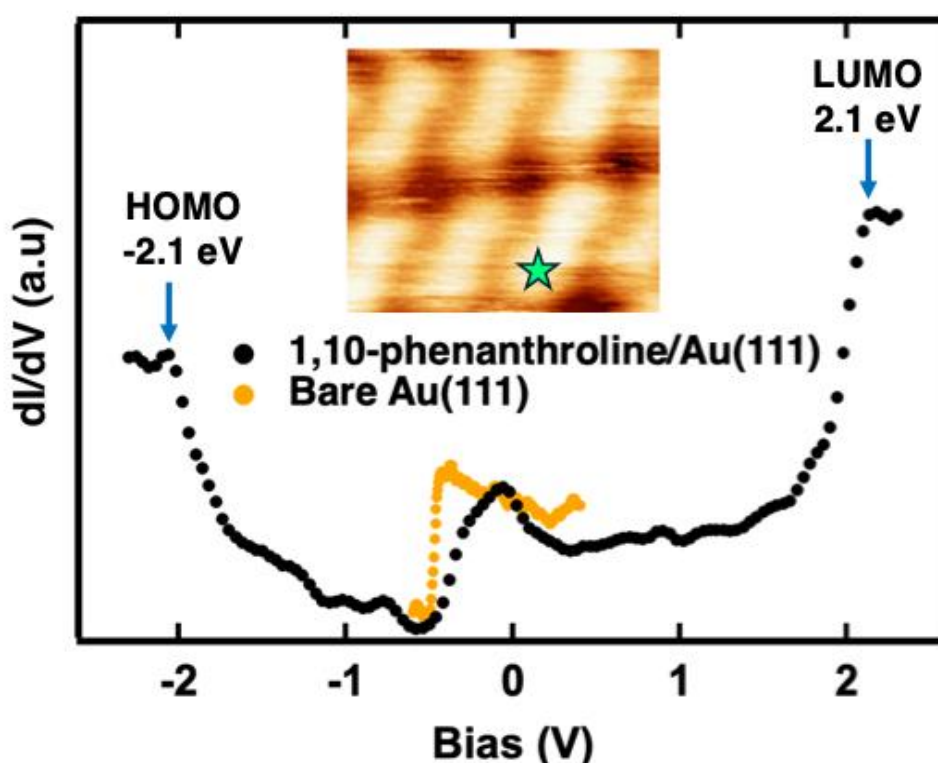


Figure 4. Differential conductance ( $dI/dV$ ) spectrum of 1,10-phenanthroline adsorbed on Au(111), shown as black circles. The spectrum was recorded above a molecule indicated by a star in the inset STM image, under the tunneling condition  $V = 2.2$  V,  $I_t = 0.1$  nA,  $V_{\text{mod}} = 20$  mV,  $f_{\text{mod}} = 912$  Hz. A spectrum of bare Au(111) is also shown as a reference (yellow circles), under the tunneling condition  $V = 401$  mV,  $I_t = 200$  pA,  $V_{\text{mod}} = 30$  mV,  $f_{\text{mod}} = 761$  Hz.



van der Waals interaction is dominant for the present molecular adsorption. The energy level is modified by the adsorption of molecules on the Au(111) surface, causing the shifting of the energy state as often seen for the molecular thin films deposited on noble metal (111) surfaces <sup>[19–22]</sup>. We also observe that the molecular array becomes less stable at higher temperatures  $\sim 77$  K, suggesting the weak physisorption of the molecules due to van der Waals interactions on the Au(111). These findings may indicate that while molecular adsorption modulates the surface state energy levels, the ordered 1,10-phen layer preserves well-defined molecular orbitals and maintains electronic decoupling from the substrate—making it a promising platform for probing redox-active sites such as pyridinic nitrogen.

### 3.3 XPS results

To evaluate the suitability of UHV-deposited 1,10-phen films on Au(111) for ex-situ characterization techniques, it is crucial to confirm that the molecular layer remains stable after air exposure. Figure 5 shows XPS spectra taken on 1,10-phen/Au(111) after several days of air exposure. Clear C 1s and N 1s peaks are visible, proving the existence of 1,10-phen molecular film on Au(111) surface even after air exposure. The N 1s peak position 399.4 eV is 0.8 eV higher than the experimentally determined binding energy 398.6 eV for pyri-N of 1,10-phen molecules/CB<sup>[12]</sup>. It is close to the calculated N1s binding energy 399.7 eV for H<sub>2</sub> attached 1,10-phen molecules<sup>[12]</sup>.

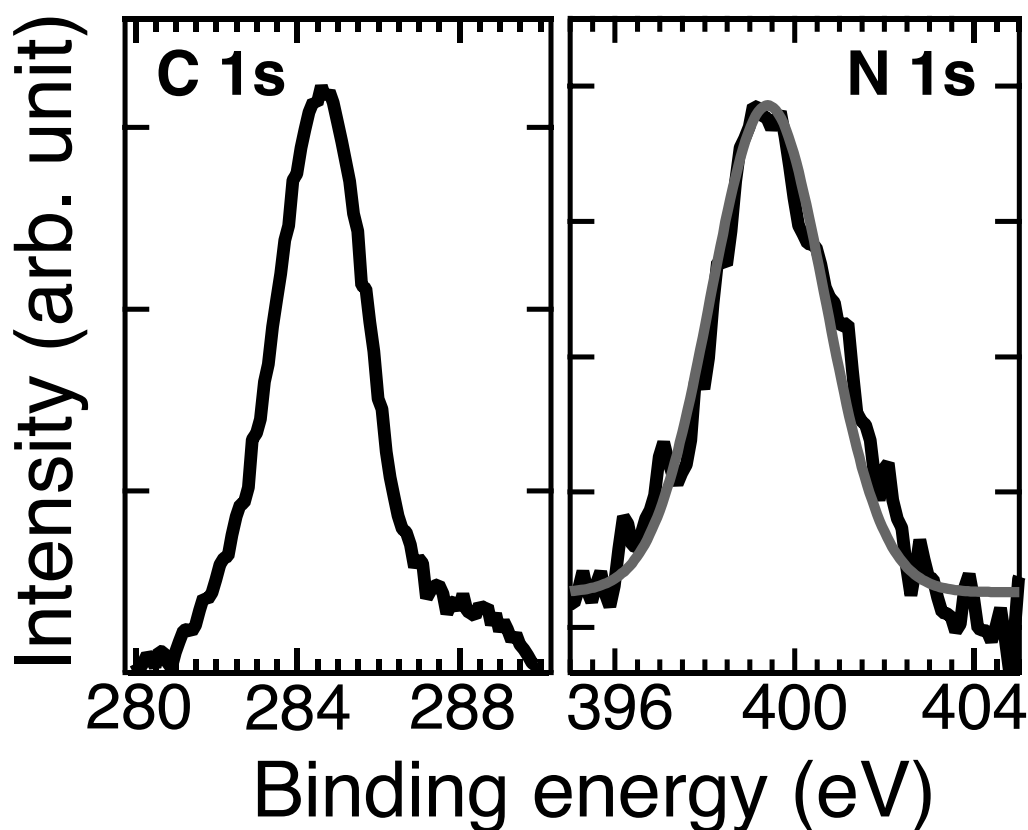


Figure 5. X-ray photoelectron spectra of 1,10-phenanthroline deposited on Au(111). C 1s is shifted so that the peak center matches to the literature value 284.6 eV, and N 1s is also shifted with the same energy offset.

However, H<sub>2</sub> has only tiny portions in the air and there is little possibility for it to react with 1,10-phen molecules. The observed energy shift likely reflects a net negative charging of the molecular film via electron transfer from the Au(111) substrate, suggesting that the electronic structure of the film remains active and may even be tuned by the substrate environment—an essential property for catalytic applications. The purpose of constructing the ORR model catalyst is to analyze the behavior of pyridinic nitrogen to elucidate the ORR mechanism. Therefore, it is significant that pyridinic nitrogen can be arranged on the Au(111) surface without any chemical interactions.

## 4 Conclusion

We have successfully grown 1,10-phen on Au(111) substrates using a vapor deposition method under UHV conditions and characterized its adsorption behavior and electronic structure by in-situ STM/STS. This bottom-up approach leads to a flat-lying molecular configuration on the Au(111) surface. It allows the pyridinic nitrogen sites to remain accessible for potential catalytic reactions unlike solution-based methods. We confirm that the molecular film stays on the Au(111) surface even after exposing to the air by XPS measurements. These findings not only clarify the adsorption geometry and electronic structure at the atomic scale but also establish a robust model platform for exploring spin-coupled proton–electron transfer mechanisms in ORR, with potential extension to other catalytic processes such as CO<sub>2</sub> activation.

## 5 Acknowledgements

We thank Noriyuki Tsukahara for technical assistance in constructing the molecular evaporator and for valuable discussions on experimental results. We also thank Kotaro Takeyasu and Kenji Hayashida for discussions and XPS measurements, and Koichi Nunomura for providing liquid Helium for low-temperature STM. This work was partially supported by Grants-in-Aid for Scientific Research from the Japan Society for the Promotion of Science (nos. 23H05459 and 23K26541) and by JST SPRING, Grant Number JPMJSP2135.

## References

- [1] D. Guo, R. Shibuya, C. Akiba, S. Saji, T. Kondo, J. Nakamura, “Active sites of nitrogen-doped carbon materials for oxygen reduction reaction clarified using model catalysts”, *SCIENCE* **2016**, *351*, 361–365.
- [2] P. Sahu, R. Mishra, S. Panigrahy, P. Panda, S. Barman, “Constructing micropore-rich nitrogen-doped carbon for high-performance supercapacitor and adsorption of carbon dioxide”, *Int. J. Energy Res.* **2022**, *46*, 13556–13569.
- [3] Q. Wu, L. Yang, X. Wang, Z. Hu, “From Carbon-Based Nanotubes to Nanocages for Advanced Energy Conversion and Storage”, *Acc. Chem. Res.* **2017**, *50*, 435–444.
- [4] A. Aijaz, N. Fujiwara, Q. Xu, “From Metal–Organic Framework to Nitrogen-Decorated Nanoporous Carbons: High CO<sub>2</sub> Uptake and Efficient Catalytic Oxygen Reduction”, *J. Am. Chem. Soc.* **2014**, *136*, 6790–6793.
- [5] H. B. Yang, J. Miao, S.-F. Hung, J. Chen, H. B. Tao, X. Wang, L. Zhang, R. Chen, J. Gao, H. M. Chen, L. Dai, B. Liu, “Identification of catalytic sites for oxygen reduction

and oxygen evolution in N-doped graphene materials: Development of highly efficient metal-free bifunctional electrocatalyst”, *Sci. Adv.* **2016**, 2, e1501122.

[6] A. S. Varela, W. Ju, P. Strasser, “Molecular Nitrogen–Carbon Catalysts, Solid Metal Organic Framework Catalysts, and Solid Metal/Nitrogen-Doped Carbon (MNC) Catalysts for the Electrochemical CO<sub>2</sub> Reduction”, *Adv. Energy Mater.* **2018**, 8, DOI 10.1002/aenm.201703614.

[7] Y. Zhao, R. Nakamura, K. Kamiya, S. Nakanishi, K. Hashimoto, “Nitrogen-doped carbon nanomaterials as non-metal electrocatalysts for water oxidation”, *Nat. Commun.* **2013**, 4, 2390.

[8] K. Gong, F. Du, Z. Xia, M. Durstock, L. Dai, “Nitrogen-Doped Carbon Nanotube Arrays with High Electrocatalytic Activity for Oxygen Reduction”, *Science* **2009**, 323, 760–764.

[9] Y. Xu, S. Wu, S. Ren, J. Ji, Y. Yue, J. Shen, “Nitrogen-doped porous carbon materials generated via conjugated microporous polymer precursors for CO<sub>2</sub> capture and energy storage”, *RSC Adv.* **2017**, 7, 32496–32501.

[10] W. Ju, A. Bagger, G.-P. Hao, A. S. Varela, I. Sinev, V. Bon, B. R. Cuenya, S. Kaskel, J. Rossmeisl, P. Strasser, “Understanding activity and selectivity of metal-nitrogen-doped carbon catalysts for electrochemical reduction of CO<sub>2</sub>”, *Nat. Commun.* **2017**, 8, 944.

[11] K. Hayashida, J. Nakamura, K. Takeyasu, “Why Does the Performance of Nitrogen-Doped Carbon Electrocatalysts Decrease in Acidic Conditions?”, *Angew. Chem. Int. Ed.* **2025**, e202502702.

[12] K. Takeyasu, M. Furukawa, Y. Shimoyama, S. K. Singh, J. Nakamura, “Role of Pyridinic Nitrogen in the Mechanism of the Oxygen Reduction Reaction on Carbon Electrocatalysts”, *Angew. Chem. Int. Ed.* **2021**, 60, 5121–5124.

[13] S. K. Singh, K. Takeyasu, K. Homma, S. Ito, T. Morinaga, Y. Endo, M. Furukawa, T. Mori, H. Ogasawara, J. Nakamura, “Activating Nitrogen-doped Graphene Oxygen Reduction Electrocatalysts in Acidic Electrolytes using Hydrophobic Cavities and Proton-conductive Particles”, *Angew. Chem. Int. Ed.* **2022**, 61, e202212506.

[14] G. Chen, M. Isegawa, T. Koide, Y. Yoshida, K. Harano, K. Hayashida, S. Fujita, K. Takeyasu, K. Ariga, J. Nakamura, “Pentagon-Rich Caged Carbon Catalyst for the Oxygen Reduction Reaction in Acidic Electrolytes”, *Angew. Chem. Int. Ed.* **2024**, 63, e202410747.

[15] G. Chen, T. Koide, J. Nakamura, K. Ariga, “Nanoarchitectonics for Pentagon Defects in Carbon: Properties and Catalytic Role in Oxygen Reduction Reaction”, *Small Methods* **2025**, e2500069.

[16] R. Shibuya, K. Takeyasu, D. Guo, T. Kondo, J. Nakamura, “Chemisorption of CO<sub>2</sub> on Nitrogen-Doped Graphitic Carbons”, *Langmuir* **2022**, 38, 14430–14438.



- [17] P. F. Cafe, A. G. Larsen, W. Yang, A. Bilic, I. M. Blake, M. J. Crossley, J. Zhang, H. Wackerbarth, J. Ulstrup, J. R. Reimers, “Chemisorbed and Physisorbed Structures for 1,10-Phenanthroline and Dipyrido[3,2-a:2',3'-c]phenazine on Au(111)”, *J. Phys. Chem. C* **2007**, *111*, 17285–17296.
- [18] S. Gümüş, A. Gümüş, “A computational study on a series of phenanthrene and phenanthroline based potential organic photovoltaics”, *Maced. J. Chem. Chem. Eng.* **2017**, *36*, 239–249.
- [19] Y. Yoshida, H.-H. Yang, H.-S. Huang, S.-Y. Guan, S. Yanagisawa, T. Yokosuka, M.-T. Lin, W.-B. Su, C.-S. Chang, G. Hoffmann, Y. Hasegawa, “Scanning tunneling microscopy/spectroscopy of picene thin films formed on Ag(111)”, *J. Chem. Phys.* **2014**, *141*, 114701.
- [20] B. W. Heinrich, L. Limot, M. V. Rastei, C. Iacovita, J. P. Bucher, D. M. Djimbi, C. Massobrio, M. Boero, “Dispersion and Localization of Electronic States at a Ferrocene/Cu(111) Interface”, *Phys. Rev. Lett.* **2011**, *107*, 216801.
- [21] T. Andreev, I. Barke, H. Hövel, “Adsorbed rare-gas layers on Au(111): Shift of the Shockley surface state studied with ultraviolet photoelectron spectroscopy and scanning tunneling spectroscopy”, *Phys. Rev. B* **2004**, *70*, 205426.
- [22] A. Sabitova, R. Temirov, F. S. Tautz, “Lateral scattering potential of the PTCDA/Ag(111) interface state”, *Phys. Rev. B* **2018**, *98*, 205429.